Electronic Supplementary Material (ESI) for Journal of Materials Chemistry A.

Electronic Supplementary Information

Au@Poly(acrylic acid) Plasmons and C_{60} improve light harvesting capability of a TiO_2/CdS/CdSeS Photoanode

P. Naresh Kumar,[a] Remya Narayanan,[a] Melepurath Deepa [a,] and Avanish Kumar Srivastava[b]*

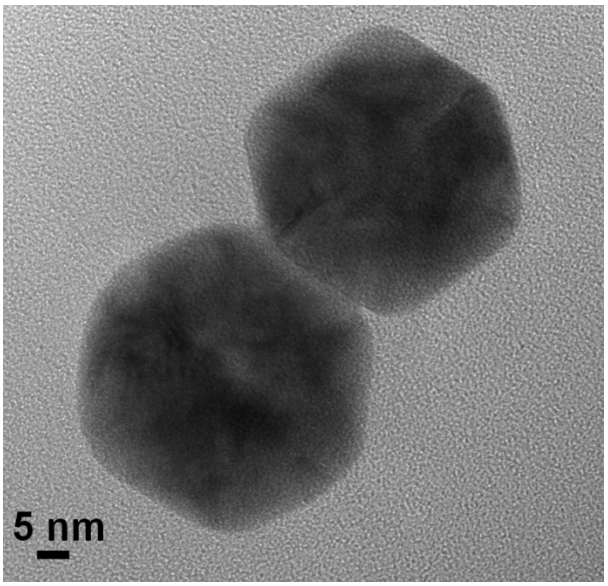

Figure S1 TEM image of Au@PAA nanoparticles, showing the hexagonal shape of the particles.

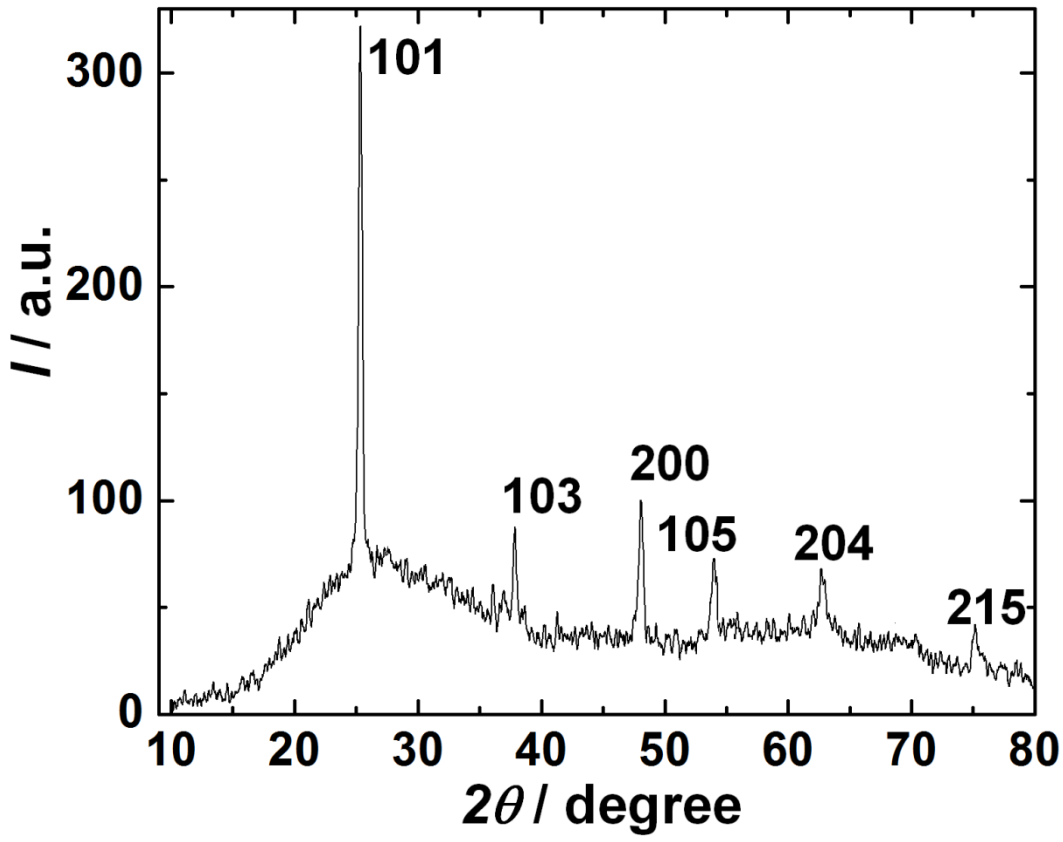

Figure S2 XRD pattern of pristine TiO_2.

The XRD pattern of pristine TiO_2 is shown in Figure S1. The pattern shows peaks at d = 3.51, 2.45, 1.89, 1.69, 1.48 and 1.26 Å which match well with the (101), (103), (200), (105), (204) and (215) planes of the body centered tetragonal crystal structure of TiO_2 respectively, as per PDF number 894921.

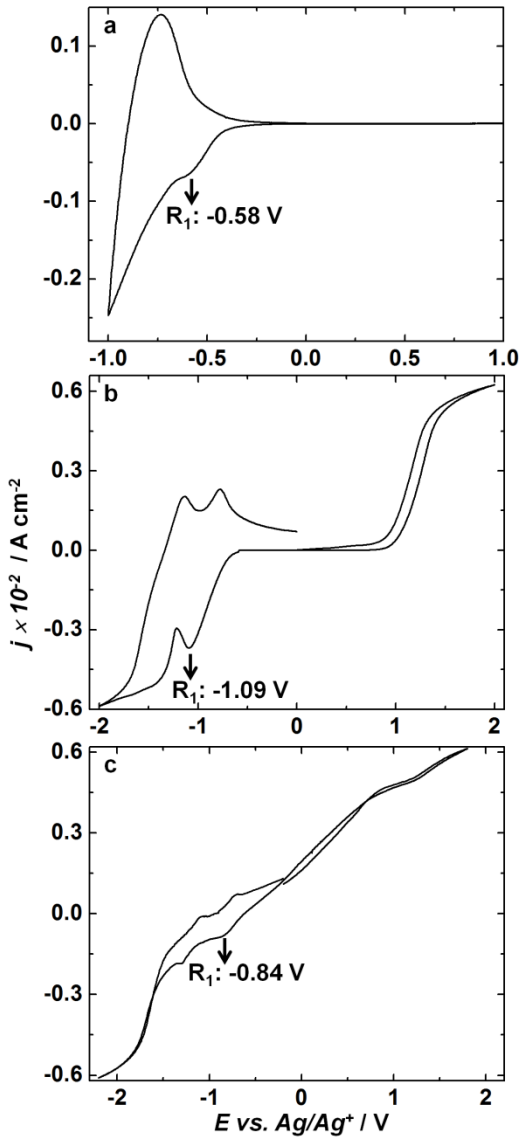

Figure S3 Cyclic voltammograms recorded at a scan rate of 5 mV s^{-1} in a 0.1 M KCl solution in three electrode electrochemical cells with (a) TiO_2/FTO, (b) CdS/FTO and (c) CdSeS/FTO as working electrodes in each case, Ag/AgCl/KCl as reference electrode and a Pt rod as the auxiliary electrode.

The cyclic voltammograms of TiO_2, CdS and CdSeS show the first reduction peak (labeled as R_1 for each electrode in Figure S2) at –0.58, –1.09 and –0.84 V (*versus* Ag/Ag^+) in their cathodic branches respectively. The potential of reference electrode (Ag/Ag^+) was +0.197 V (*versus*

NHE). The reduction potential (*versus* NHE) corresponds to the LUMO of the electroactive material.

Therefore, the reduction potential of TiO_2 (*versus* NHE) will be: E_R = (–0.58 + 0.197) V = –0.383 V. Similarly, the reduction potential of CdS (*versus* NHE) will be: E_R = (–1.09 + 0.197) V = –0.893 V and that of CdSeS (*versus* NHE) will be: E_R = (–0.84 + 0.197) V = –0.643 V. A potential of 0 V (*versus* NHE) corresponds to 4.5 eV (w.r.t. vacuum level). The LUMO or CB positions of TiO_2, CdS and CdSeS were therefore calculated to be 4.12, 3.61 and 3.86 eV and these values were used in the energy band diagram shown in Figure 5.

Determination of equilibrated Fermi level in the TiO_2/CdS/CdSeS/C_{60}/Au@PAA electrode

In KPFM, an ac bias is applied to a conducting Pt/Ir tip of a known work function, it scans the sample (TiO_2/CdS/CdSeS/C_{60}/Au@PAA) surface and the localized contact potential difference (V_{CPD}) that arises between the conducting tip and the sample surface, is used for generating the surface potential map, as shown in the following equation.

$$V_{CPD} = (\Phi_{tip} - \Phi_{sample}) / e^{-} \quad (1)$$

Φ_{tip} is the work function of the conducting Pt/Ir coated Si cantilever (5.5 eV) and Φ_{sample} is the work function of the sample, i.e. the TiO_2/CdS/CdSeS/C_{60}/Au@PAA electrode, which can be approximated to its' Fermi level position. The work function of Pt/Ir tip was first calibrated with highly ordered pyrolytic graphite (HOPG) (Φ_{HOPG} = 4.6 eV) to convert the measured V_{CPD} to absolute surface work function. The absolute surface work function of the sample was calculated with equation (2).

$$\Phi_{sample} = 4.6 \text{ eV} + V_{CPDHOPG} - V_{CPDsample} \quad (2)$$

In KPFM, the topography of the film surface is measured in tapping mode and the surface potential variation is measured with conducting tip. The tip was held at ~100 nm above the film

surface, and it is charged due to the applied ac potential. The sample surface is also charged since it is in the vicinity of the charged tip. The surface potential of the TiO_2/CdS/CdSeS/C_{60}/Au@PAA assembly was 300 mV and the corresponding work function calculated using equation (2) was 4.7 eV. KPFM was performed on the electrode using a Veeco, Multimode 8 with ScanAsyst (Nanoscope 8.10 software) microscope. The conductive probe used herein was coated with Pt/Ir on front and back sides. The probe tip had a radius of 10 nm, spring constant of 0.2 N cm^{-2}, a current sensitivity of 1 nA V^{-1} and a load force of 50 nN was maintained between the tip and the sample. The sample deposited on FTO coated glass was affixed on a stainless steel disk with a conducting carbon tape. A thin strip of pin-hole free silver paste was used for taking contacts. The equilibrated Fermi level position of the photoanode is 4.7 eV, which was used in Figure 5.

Reason for using a methanol based electrolyte

The methanol:water ratio for electrolyte was optimized on the basis of J-V characteristics. As an illustrative example, the J-V characteristics of a TiO_2/CdS cell recorded in a 0.1 M aqueous Na_2S and 0.1 M water:methanol (3:7 v/v) are shown (Figure S4). The efficiency of the cell with in an aqueous electrolyte was 1.95 and that of the cell in a methanol based electrolyte was 2.14, thus validating the use of methanol based electrolyte.

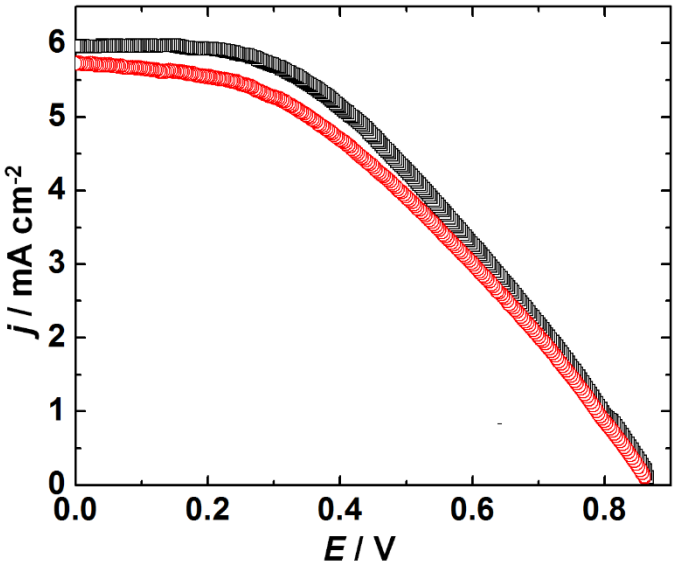

Figure S4 J-V characteristics of a photoelectrochemical solar cell with a TiO_2/CdS photoanode: in a 0.1 M Na_2S in ultrapure water/methanol 3:7 v/v solution (⭘) and in a 0.1 M Na_2S in ultrapure water solution (ᔓ). Measurements were performed under 1 sun illumination and at $\lambda >$ 300 nm and a MWCNT/FTO assembly was used as a counter electrode.

Table S1 J-V characteristics of the cell with TiO_2/CdS photoanode with two different electrolytes

Photoanode configuration	V_{OC} (V)	J_{SC} (mA cm^{-2})	FF	η (%)
In 0.1 M Na_2S in ultrapure water/methanol 3:7 v/v	0.867	5.96	41.41	2.14
In a 0.1 M Na_2S in ultrapure water	0.862	5.725	39.76	1.95

The use of methanol in the electrolyte does not also cause any V_{OC} decay. The V_{OC} was fairly stable, upon prolonged exposure to the electrolyte. This was confirmed by measuring J-V characteristics of a TiO_2/CdS cell before and after 48 h exposure to a S^{2-} electrolyte (Figure S5). The V_{OC} before exposure was 867 mV and after exposure, it was 835 mV.

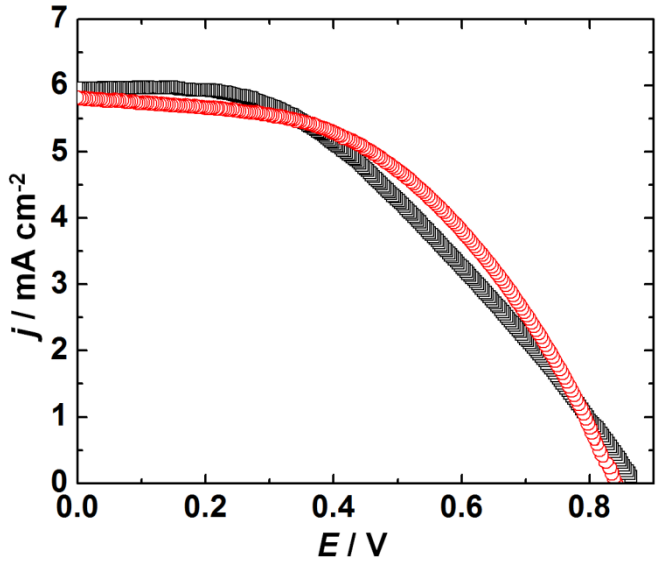

Figure S5 J-V characteristics of a photoelectrochemical solar cell with a TiO_2/CdS photoanode: initial (●) and after 48 h in a S^{2-} electrolyte (ᔓ). Measurements were performed under 1 sun illumination and at $\lambda > 300$ nm; a 0.1 M Na_2S in ultrapure water/methanol 3:7 v/v solution was employed as the electrolyte and a MWCNT/FTO assembly was used as a counter electrode.

Table S2 J-V characteristics of the cell with TiO_2/CdS photoanode

Photoanode configuration	V_{OC} (V)	J_{SC} (mA cm^{-2})	FF	η (%)
TiO_2/CdS (initial)	0.867	5.96	41.41	2.14
TiO_2/CdS (after 48 h in S^{2-} electrolyte)	0.835	5.8	48.73	2.35

Table S3 Performance parameters of similar solar cells (data from literature)

Photoanode, counter electrode (CE) configurations	V_{OC} (V)	J_{SC} (mA cm^{-2})	FF	η (%)	Reference
TiO_2/CdS CE: MWCNTs	0.867	5.96	41.41	2.14	This work

TiO_2/CdS/CdSeS/C_{60}/Au@PAA CE: MWCNTs	0.756	9.84	48.48	3.61	This work
CdS/TiO_2 (Microwave assisted chemical bath deposition), CE: Au/FTO	0.46	7.20	35	1.18	[1]
CdS nanorod-TiO_2 nanowires (chemical vapor deposition)	0.74	4.85	42	1.51	[2]
CdS-TiO_2/CdSe-TiO_2 (in paint form), CE: Cu_2S/reduced graphene oxide	0.585	3.1	59	1.18	[3]
CdS/ZnS/TiO_2 (varying cationic baths, using SILAR) CE: Cu_2S on brass foil	0.54	9.49	42	2.15	[4]
Orange and red CdSeS/TiO_2 (electrophoretic deposition of capped CdSeS) CE: Cu_2S/reduced graphene oxide	0.557	11.2	51	3.20	[5]
CdS (by SILAR) CE: Cu_2S/reduced graphene oxide	0.496	7.2	46	1.63	[6]
Poly(3-hexylthiophene) modified CdS@TiO_2 shell-core nanorod array (By hydrothermal and electrochemical methods) CE: Pt/FTO	0.726	4.3	44.3	1.38	[7]
TiO_2/Pbs/CdS (By SILAR) CE: Cu_2S/Brass	0.295	7.08	53.34	1.11	[8]

Effect of electrolyte on TiO_2/CdS/CdSeS/C_{60}/Au@PAA electrode's performance

Uncapped Au particles will have a stronger propensity to form sulfides, when brought in contact with a S^{2-} electrolyte solution. The presence of the PAA cap, inhibits the interaction between Au and S^{2-} as we did not observe any significant change in the solar cell parameters, when the TiO_2/CdS/CdSeS/C_{60}/Au@PAA electrode was kept immersed in the S^{2-} solution for 48 h in a dessicator, and J-V characteristics were measured again (Figure S6, Table S4).

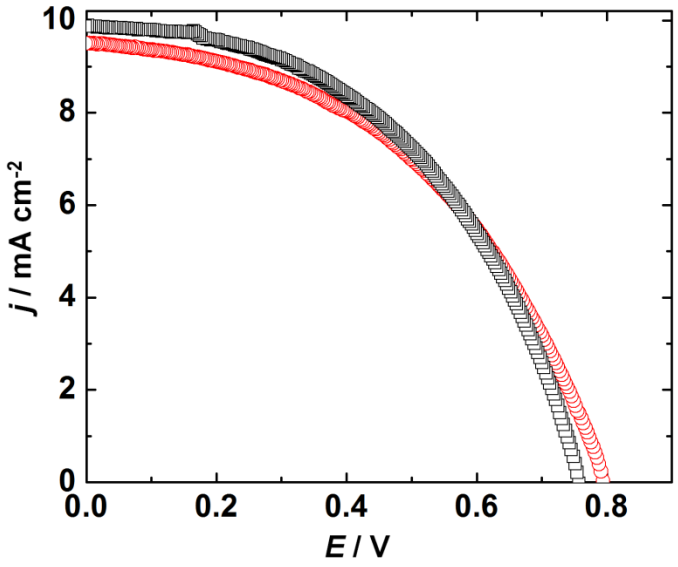

Figure S6 J-V characteristics of a photoelectrochemical solar cell with a TiO_2/CdS/CdSeS/C_{60}/Au@PAA photoanode: initial (●) and after 48 h in a S^{2-} electrolyte (ᔓ). Measurements were performed under 1 sun illumination and at $\lambda > 300$ nm; a 0.1 M Na_2S in ultrapure water/methanol 3:7 v/v solution was employed as the electrolyte and a MWCNT/FTO assembly was used as a counter electrode.

Table S4 J-V characteristics of the cell with TiO_2/CdS/CdSeS/C_{60}/Au@PAA photoanode

Photoanode configuration	V_{OC} (V)	J_{SC} (mA cm^{-2})	FF	η (%)
TiO_2/CdS/CdSeS/C_{60}/Au@PAA (initial)	0.756	9.84	48.48	3.61
TiO_2/CdS/CdSeS/C_{60}/Au@PAA (after 48 h in S^{2-} electrolyte)	0.795	9.48	46.50	3.50

References

1. G. Zhu, L. Pan, T. Xu and Z. Sun, *ACS Appl. Mater. Interfaces,* 2011, **3,** 1472–1478.
2. J. C. Lee, T. G. Kim, W. Lee, S. H. Han and Y. M. Sung, *Crys. Growth Des.,* 2009, **9,** 4519–4523.
3. M. P. Genovese, I. V. Lightcap and P. V. Kamat, *ACS Nano*, 2012, **6,** 865–872.

4. R. Zhou, Q. Zhang, J. Tian, D. Myers, M. Yin and G. Cao, *J. Phys. Chem. C,* 2013, **117,** 26948−26956.
5. P. K. Santra and P. V. Kamat, *J. Am. Chem. Soc.,* 2013, **135,** 877−885.
6. P. K. Santra and P. V. Kamat, *J. Am. Chem. Soc.*, 2012, **134,** 2508−2511
7. Y. Li, Y. Hao, S. Sun, B. Sun, J. Pei, Y. Zhang, D. Xu and L. Liu, *RSC Adv.,* 2013, **3,** 1541–1546.
8. Md. A. Hossain, Z. Y. Koh and Q. Wang, *Phys. Chem. Chem. Phys.*, 2012, **14,** 7367–7374.